

Active Cancellation of Hostile RADAR Sources in Conformal Array

Hema Singh, Neethu P.S., and Mausumi Dutta

Centre for Electromagnetics (CEM)
CSIR-National Aerospace Laboratories
Bangalore 560017, India

Abstract—The onboard antennas contribute significantly to the overall radar signatures of aerospace structures such as aircraft and missiles. The interference suppression capability of phased arrays can be exploited towards radar cross section (RCS) reduction. In this paper, the probe suppression in dipole array placed over a finite right circular cylinder is shown. The modified improved LMS algorithm is used to obtain optimum antenna weights and hence the adapted pattern for an arbitrary signal environment. The effect of platform and mutual coupling effect is included. The antenna elements placed over a non-planar platform is dealt using Euler's transformation for obtaining array manifold for a given signal scenario. Results are presented for both conducting and dielectric cylinder. It is shown that the dipole array is able to cater to an arbitrary signal environment by maintaining mainlobe towards each of the desired source and suppressing the probing sources.

Index Terms—Cylindrical dipole array, Euler rotation, Modified Improved LMS algorithm, Probe suppression, Platform effect, Mutual coupling.

I. INTRODUCTION

One of the important issues faced by antenna engineers in designing antenna array systems mounted on a finite platform is the current that flows over the surface. This surface current substantially affects the radiation characteristics of the array. In most of the aerospace structures, the platform is more or less cylindrical in shape. This allows approximating the structures as a finite cylinder. The far-field radiation pattern of dipole placed near an infinite conducting cylinder has been derived using the principle of reciprocity [1]. The corresponding analysis for finite conducting cylinder was reported by Kuehl [2]. The portions of the infinite cylinder above and below the cylindrical section considered were ignored with the assumption that the current on the remaining portion of the cylinder remain unchanged. The far-field of this unchanged portion of the current was added to the dipole field to arrive at the far-field radiation pattern of a dipole antenna placed very close to the cylinder.

Furthermore, the presence of a metallic platform near a radiating dipole antenna results in significant reduction in its radiation resistance. The real and imaginary part of the antenna impedance drops when the antenna is in close vicinity to the platform [3]. If the platform is a dielectric cylinder, scattering due to the surface of a cylinder introduces a back scattering lobe in the radiation pattern, reducing the amplitude of forward scattering. This effect is more prominent when the dipole antenna is placed very close to the cylinder [4]. If the

radius of a dielectric cylinder is comparable to the wavelength, the dipole element placed close to it can be used as a means of directing the field in the back lobe of the radiation pattern. Similar observations have been reported for dipole antenna placed within the dielectric cylinder [5].

The finite element-boundary integral (FE-BI) method has been employed to model the scattering and radiation of cavity-backed patch antennas [6]. The metallic cylinder as a platform is reported to have improved gain as compared to dielectric cylinder. Another approach to analyze the effect of platform on the antenna performance is to include directivity factors in continuous current distribution of dipole array placed over a conducting cylinder [7].

The ray theoretic methods such as geometrical theory of diffraction (GTD), uniform theory of diffraction (UTD), physical theory of diffraction (PTD) have been employed to analyze the radiation characteristics of slot and dipole antennas over convex conducting surfaces [8]. In recent years, the hybrid methods combining ray-based asymptotic method and numerical techniques are preferred choice for antenna analysis. The field components on the closed surface enclosing the antenna are computed by numerical technique-based methods such as method of moments (MoM) and the scattered fields from the platform in far-field region are determined using high-frequency techniques such as UTD [9]. The reciprocity theorem in conjunction with MoM is also applied to evaluate the radiated fields from the microstrip patch antenna on cylindrical platforms [10].

In this paper, a uniform array of centre-fed dipole array is considered to be placed over a finite right circular cylinder. Multiple narrowband signals are assumed to impinge the array from different directions. Euler rotation-based method is used to extract elevation and azimuth angles for each antenna element location on the cylinder. Accordingly the steering vector i.e. array manifold for a given signal scenario consisting of both desired and probing sources is determined. A modified improved least mean square (LMS) algorithm [11] is used for the weight adaptation and hence the generation of quiescent and adapted patterns. Results are presented for dipole array placed on conducting and dielectric cylinder. It is known that if multiple antennas share the same ground plane, surface currents can cause unwanted coupling between the antennas. Here, the mutual coupling effect on the array performance is taken into account. It is shown that cylindrical dipole array efficiently cater to the signal scenario by efficiently suppressing each probing source and maintaining the mainlobes towards the desired sources. The probe suppression in hostile probing directions makes the array

invisible to the probing sources. This suppression capability of array once integrated with the structural and radiation mode radar cross section (RCS) of array mounted over a platform will significantly control the RCS of the platform in hostile signal environment.

II. RADIATION CHARACTERISTICS OF DIPOLE ARRAY OVER CONDUCTING PLATFORM

A dipole antenna placed on a surface, whether conducting or non-conducting radiates differently, as compared to its free-space radiation pattern.

For example, when two vertical dipoles are placed over a conducting right circular cylinder, the radiated field is given by [1]

$$E'_\theta = \sin \theta [2C_0 + 4C_2 \cos 2\phi + 4C_4 \cos 4\phi + \dots]. \quad (1)$$

$$C_n = J_n(x_2) - \{J_n(x_1)/U_n(x_1)\}U_n(x_2). \quad (2)$$

$$x_1 = k_o R \sin \theta. \quad x_2 = k_o R_1 \sin \theta. \quad (2a)$$

where, R is radius of cylinder, R_1 is the distance of dipole antenna from the cylinder axis, U_n is n^{th} order Hankel function of second kind, J_n is n^{th} order Bessel function.

Figure 1 shows the radiation pattern of two vertical dipole antennas placed diametrically opposite around a conducting right circular cylinder. The dipoles are placed at a distance of 0.5λ from the cylinder of radius 5λ .

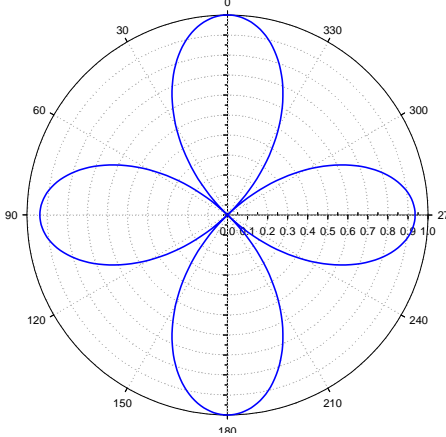


Fig.1. Radiation pattern of two dipole antennas placed diametrically opposite position over a right circular conducting cylinder

For a dielectric cylinder, the platform effect varies due to the constitutive parameters of the surface over which antenna array is placed [1]. The details of radiation pattern of dipole antenna over dielectric cylinder can be referred to [1], [13].

III. ACTIVE CANCELLATION OF HOSTILE RADAR SOURCES IN CONFORMAL ARRAY

In conformal array analysis, due to non planar surface transformation of antenna pattern from local coordinate to global coordinate is required. The coordinates of antenna

elements are extracted using Euler's transformation. The modified improved LMS algorithm [11] is used for calculating optimal weights so as to actively cancel radar sources. Adapted weights are calculated in the presence of mutual coupling between antenna elements and platform effect.

In non-planar array, the steering vector may be expressed in global coordinate system [12] as

$$S_{\theta\phi} = \sum_{n=1}^N E'_\theta \exp(j k_o r_n \cdot v). \quad (3)$$

E'_θ represents the element pattern in the global cartesian coordinate system, $r_n = [x_n, y_n, z_n]$ is the position vector from the origin to the center of the n^{th} antenna element and $v = [\sin \theta \cos \phi, \sin \theta \sin \phi, \cos \theta]^T$ is unit radial vector from the coordinate origin to the observation point.

In Euler's rotation method, the Euler transformation matrix is derived by three successive rotations ($\alpha_1, \alpha_2, \alpha_3$) of the coordinate axes. In the first rotation, the x - and y -axes are rotated about z -axis by an angle α_1 . Then x' and z' axes are rotated by an angle α_2 keeping y' -axis fixed. In the third rotation, the axes are rotated by angle α_3 w.r.t. z'' axis. The unit vector pointing in the direction of (θ, ϕ) in global coordinates is expressed as

$$[x \ y \ z] = [\sin \theta \cos \phi \ \sin \theta \sin \phi \ \cos \theta]. \quad (4)$$

Next, the transformation from global coordinate (θ, ϕ) to local coordinate $(\tilde{\theta}_i, \tilde{\phi}_i)$ gives

$$[\tilde{x} \ \tilde{y} \ \tilde{z}]^T = E(\alpha_1, \alpha_2, \alpha_3) [x \ y \ z]^T. \quad (5)$$

The corresponding elevation and azimuth angles $(\tilde{\theta}_i, \tilde{\phi}_i)$ based on antenna element position on the surface in local coordinates are extracted as

$$\tilde{\theta}_i = \cos^{-1}(\tilde{z}); \quad \tilde{\phi}_i = \tan^{-1}\left(\frac{\tilde{y}}{\tilde{x}}\right). \quad (6)$$

These elevation and azimuth angles are substituted in E'_θ to obtain the radiation pattern of dipole antenna element placed over a circular cylinder of radius R . A uniform inter-element spacing d is considered. The array elements are placed along a circular arc.

Towards array processing, the total received signal by dipole array for a multiple signal scenario, is given by

$$x_{n\theta\phi} = \sum_k S_{o\theta\phi} S_{d_k} + \sum_j S_{p\theta\phi} i_{p_j} + T_n. \quad (7)$$

Here $S_{o\theta\phi}$ and $S_{p\theta\phi}$ are the steering vectors for desired signals S_{d_q} , and the probing signals i_{p_j} respectively, q is the number of desired signal, j is the number of probing signals and T_n is the thermal noise in the array system. The optimal antenna excitations are obtained using modified improved LMS algorithm. In this algorithm the Toeplitz structure of the received signal covariance matrix is exploited to obtain distinct eigen values and eigen vectors for a given signal scenario. This facilitates to get converged output signal-

to-interference ratio and hence desired adapted pattern. The antenna weights are iteratively determined as

$$w(l+1) = P[w(l) - \mu \nabla(l)] + \frac{S_{o_1}}{S_{o_1}^H S_{o_1}} + \frac{S_{o_2}}{S_{o_2}^H S_{o_2}} + \dots + \frac{S_{o_q}}{S_{o_q}^H S_{o_q}}. \quad (8)$$

Where μ is the step-size, l is the snapshot and the projection operator, P for multiple desired signals is given by

$$P = I - \frac{S_{o_1} S_{o_1}^H}{S_{o_1}^H S_{o_1}} - \frac{S_{o_2} S_{o_2}^H}{S_{o_2}^H S_{o_2}}, \dots, - \frac{S_{o_m} S_{o_m}^H}{S_{o_m}^H S_{o_m}} \quad (8a)$$

where in, $S_{o_1}, S_{o_2}, \dots, S_{o_q}$ represent the steering vectors towards q desired signals impinging the array at different angles, I is the identity matrix, ∇ is the gradient vector, given by

$$\nabla(l) = 2 \tilde{R}_T(l+1)w(l). \quad (9)$$

The signal covariance matrix $\tilde{R}_T(l)$ is expressed as

$$\tilde{R}_T(l) = \frac{1}{N} x x^H. \quad (10)$$

This covariance matrix is updated with snapshots, given by

$$\tilde{R}_T(l+1) = \frac{1}{l+1} [\tilde{R}_T(l) + \hat{R}_T(l+1)]. \quad (11)$$

The adapted beam pattern for a given signal environment is obtained from the product of optimal weights and the array response, i.e.

$$pattern = 20 \cdot \log_{10}(w^H \cdot S). \quad (12)$$

The output *signal-to-interference-noise* ratio (SINR) of the array is given by

$$output \ SINR = \frac{w^H R_T w - w^H R_N w}{w^H R_N w}. \quad (13)$$

R_N is the noise correlation matrix, w^H is the Hermitian of the antenna weight vector.

Figure 2 shows the variation of output SINR with snapshots for a 16-element dipole array placed over a conducting right circular cylinder for one desired (0° ; 1) and one probing source (40° ; 1000). It is assumed that the direction of arrival (DoA) of the impinging signals are known *a priori*. It is apparent from the Figure 2 that the output SINR converges to significantly high value. This facilitates the generation of the adapted pattern according to the signal scenario. Furthermore, this high output SINR and good convergence rate establishes the efficacy of modified improved LMS algorithm used for active cancellation of hostile radar sources in conformal dipole array.

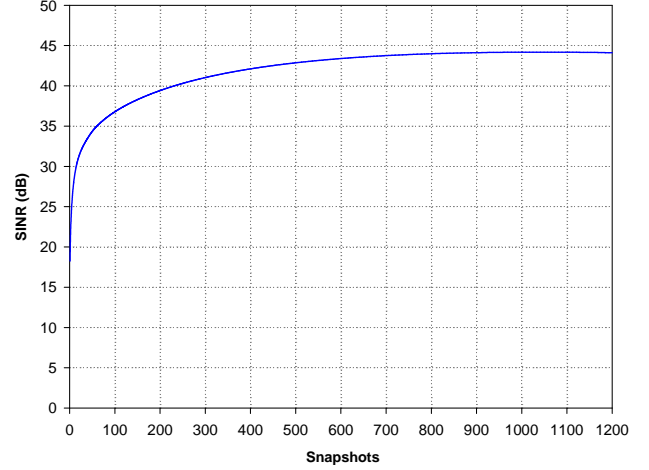


Fig. 2. Output signal-to-interference-noise ratio of a 16-element dipole array placed over a conducting cylinder. One desired signal (0° ; 1) and one probing source (40° ; 1000).

IV. RESULTS AND DISCUSSION

In this section, the simulation results of adapted pattern of cylindrical dipole array for different signal environments are presented. A uniform 16-element linear dipole array is mounted on conducting/dielectric finite cylinder. The ability of dipole array to steer the beam towards the desired sources, with acceptable sidelobe level (SLL) and minimal power transmitted in the probing direction is demonstrated. The operating frequency is 10 GHz. The antenna elements are placed within 120° sector with uniform half-wavelength inter-element spacing. The radius of the cylindrical array is taken as 5λ . The mutual coupling is taken into account. The adapted pattern is compared with the quiescent pattern for a given signal scenario. The green arrow indicates the desired source and the red arrow represents the probing source in the pattern.

A. Non-conducting Platform

The radiation and scattering characteristics of antenna array depend on the material properties of the platform. If the platform over which antenna mounted is non conducting both lobes of the dipole antenna radiation pattern change due to interference between waves reflected from the platform.

Here, platform is considered as a right circular dielectric cylinder ($\sigma = 1.2S$, $\epsilon_r = 9$). Figure 3 presents the adapted and quiescent patterns for two desired (-40° , 50° ; 1) and one probing source (20° ; 1000). It may be seen that adapted pattern maintains distortion less mainlobes and accurate null towards the probing source. This makes the array invisible to the hostile radar source attempting to probe the array.

As a next case, two desired signals (0° , 40°) each with a power ratio of 1 are assumed to impinge the array. The probing sources are at -30° and -20° with a power ratio of 1000. In adapted pattern the mainlobes are efficiently maintained towards each of the desired sources. At the same time, the probing source is actively suppressed (Figure 4).

algorithm in catering an arbitrary signal scenario even when platform effect and mutual coupling effect is taken into account.

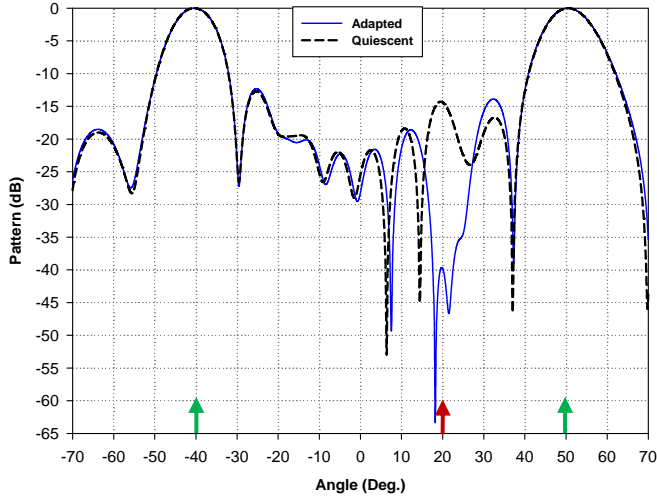


Fig. 3. Adapted pattern of a 16-element cylindrical dipole array; two desired signal (-40° , 50° ; 1 each) and one probing source (20° , 1000)

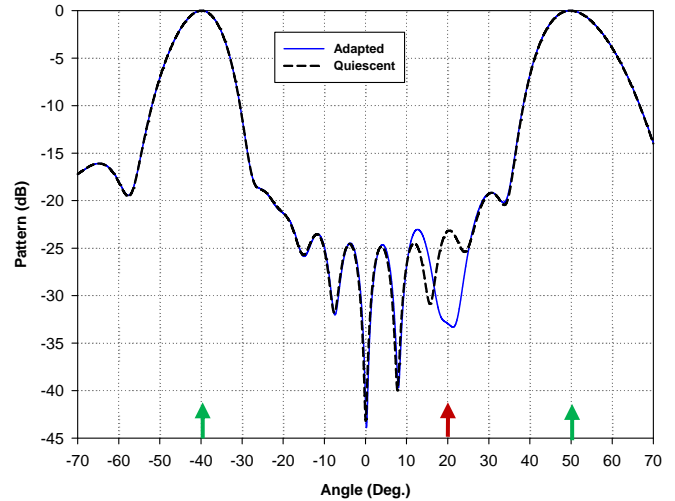


Fig. 5. Adapted pattern of a 16-element cylindrical dipole array; two desired signals (-40° , 50° ; 1 each) and one probing source (20° ; 1000)

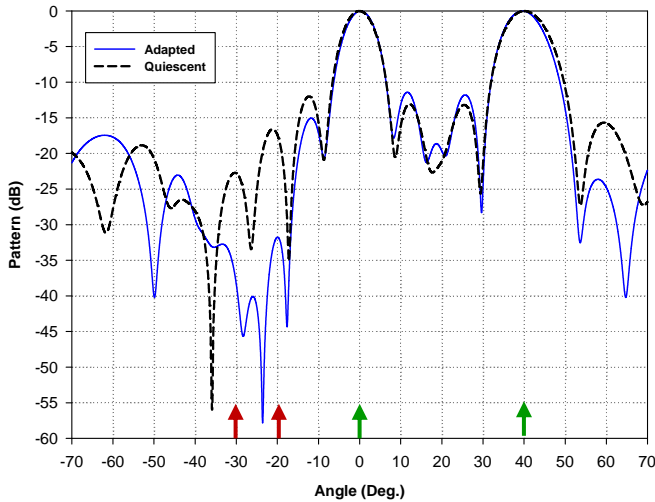


Fig. 4. Adapted pattern of a 16-element cylindrical dipole array; two desired signals (0° , 40° ; 1 each) and two probing sources (-20° , -30° ; 1000 each)

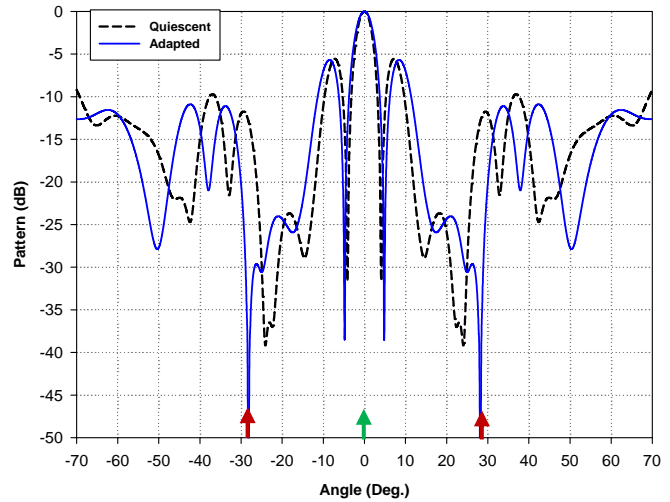


Fig. 6. Adapted pattern of a 16-element cylindrical dipole array; one desired signal (0° ; 1) and two probing sources (-28° , 28° ; 1000)

B. Conducting Platform

In this sub-section, the cylindrical surface is taken as conducting. A signal scenario of two desired sources (-40° , 50° ; 1 each) and one probing source (20° ; 1000) is considered to impinge a 16-element dipole array placed over a finite cylinder. The resultant adapted pattern in Figure 5 shows a deep null in the probing direction. The mainlobes point in the desired signal directions without any distortion.

Next, the number of probing sources is increased to two. Figure 6 shows the adapted pattern of a 16-element cylindrical dipole array for one desired sources (0° ; 1 each) and two probing sources (-28° , 28° ; 1000 each). The dipole array maintains its steering capability with distortionless mainlobes towards each of the desired sources, and simultaneously actively cancelling out both the probing sources. This demonstrates the capability of modified improved LMS

V. CONCLUSION

This paper establishes the difference in the performance of dipole array when it is placed over a conducting and dielectric platform. The effect of platform over which array is mounted alters the both the radiation and scattering characteristics of antenna array. In this paper, an efficient algorithm named modified improved LMS algorithm is employed to achieve probe suppression in conformal dipole array. The effect of platform and mutual coupling on the radiation characteristics of dipole array placed over a right circular cylinder is taken into account. The Euler transformation is used to calculate the steering vector of array mounted on a non-planar surface. The

results are presented for both conducting and dielectric cylinders. The quiescent and adapted patterns of cylindrical dipole array are shown for different signal scenarios consisting of multiple desired and probing sources. For each signal scenario, the adapted pattern maintains mainlobe towards each of the desired sources with accurate and sufficiently deep nulls in the probing directions. It is shown that the conformal array along with the algorithm is able to actively cancel the hostile probing sources without any distortion in mainlobes towards the desired directions. If this capability is integrated with the structural radar cross section of the antenna array and the platform can contribute significantly towards low observable platforms.

REFERENCES

- [1] P. S. Carter, "Antenna around cylinders," *Proceedings of IRE*, vol. 31, pp. 671-693, Dec. 1943.
- [2] H. H. Kuehl, "Radiation from a radial electric dipole near a long finite cylinder," *IRE transactions on Antennas and Propagation*, vol. 9, pp. 546-553, Nov. 1965.
- [3] X. Qing, Z.N. Chen, and C.K. Goh, "Platform effect on RFID tag antennas and co-design considerations," in *Proceedings of Asia Pacific Microwave Conference*, Macau, 2008, pp.16-20, (doi: 10.1109/APMC.2008.4958390).
- [4] G. N. Tsandoulas, "Scattering of dipole field by finitely conducting and dielectric circular cylinders," *IEEE Transactions on Antennas and Propagation*, vol. AP-16, pp. 324-328, May 1968.
- [5] R. J. Lytle, "Far- field patterns of point sources operated in the presence of dielectric circular cylinders," *IEEE Transactions on Antennas and Propagation*, vol. AP-19, no. 5, pp. 618-621, Sept. 1971.
- [6] R.J. Burkholder, P.H. Pathak, K. Sertel, R.J. Marhefka, J.L. Volakis, and R.W. Kindt, "A hybrid framework for antenna/platform analysis," *Applied Computational Electromagnetic Society Journal*, vol. 21, no. 3, pp. 177-195, November 2006.
- [7] J.E. Walsh, "Radiation patterns of arrays on a reflecting cylinder," *Proceedings of IRE*, vol. 39, pp. 1074-1081, September 1951.
- [8] P.H. Pathak, and R.G. Kouyoumjian, "An analysis of the radiation from apertures in curved surfaces by the geometrical theory of diffraction," *Proceedings of IRE*, vol. 62, pp. 1438-1447, no. 11, November 1974.
- [9] Z.L. He, K. Huang, and C.H. Liang, "Analysis of complex antenna around electrically large platform using iterative vector fields and UTD method," *Progress In Electromagnetics Research M*, vol. 10, pp. 103-117, 2009.
- [10] M. Jin, J.A. Berrie, R. Kipp and S.W. Lee, Calculation of Radiation Patterns of Microstrip Antennas on Cylindrical Bodies of Arbitrary Cross Section, Electromagnetic Scattering from Realistic Targets, Final Report, NASA NAG 3-1474, 97p., May-1997.
- [11] H. Singh and R.M. Jha, *Active Radar Cross Section Reduction: Theory and Application*. Cambridge University Press, UK, ISBN: 9781107092617, 325 p., 2015.
- [12] L. C. Godara, *Smart Antennas*. CRC Press, Washington D C, ISBN: 0-8493-1206-X, 448 p., 2004.
- [13] Mausumi Dutta, Neethu P.S., Hema Singh, and R.M. Jha, *Probe Suppression in Dipole Array Mounted on a Right Circular Cylinder*. CSIR-National Aerospace Laboratories, Bangalore, India, *Project Document PD-CEM/2015/1015*, 22 p., June 2015.



Dr Hema Singh is a Senior Scientist at the Centre for Electromagnetics of CSIR-National Aerospace Laboratories, Bangalore, India. Earlier, she was Lecturer in EEE, BITS, Pilani, India during 2001-2004.

She obtained her Ph.D. degree in Electronics Engineering from IIT-BHU, Varanasi India in 2000. Her active area of research is computational electromagnetics for aerospace applications. More specifically, the topics she has contributed to, include EM analysis of propagation in an indoor environment, Phased Arrays, Conformal Antennas, Radar Cross Section (RCS) Studies including Active RCS Reduction. She received Best Woman Scientist Award in CSIR-NAL, Bangalore for period of 2007-2008 for her contribution in area of phased antenna array, adaptive arrays, and active RCS reduction. Dr. Singh has co-authored one book, one book chapter, and over 120 scientific research papers and technical reports.



Ms. Neethu P.S. obtained B.Tech. (ECE) and M.Tech. in Communication Engineering from University of Calicut, Kerala, India. She is a Project Scientist at the Centre for Electromagnetics (CEM) of CSIR-National Aerospace Laboratories, Bangalore. Her research area includes probe suppression in phased arrays on planar and non-planar surfaces, and RCS studies for aerospace vehicles.



Ms. Mausumi Dutta is currently pursuing MTech (4th semester) in RF & Microwave Engineering from RV College of Engineering, Visvesvaraya Technological University Bangalore. She is doing her MTech. project in Centre for Electromagnetics, CSIR-National Aerospace Laboratories, Bangalore. Her research interests include probe suppression in phased arrays on planar and non-planar surfaces, and RCS studies for aerospace vehicles.